*Progress In Electromagnetics Research, Vol. 131, 117–134, 2012*

# REDUCING THE ARRAY SIZE FOR DOA ESTIMATION BY AN ANTENNA MODE SWITCH TECHNIQUE

**S.-C. Cheng and K.-C. Lee***

Department of Systems and Naval Mechatronic Engineering, National Cheng-Kung University, Tainan 701, Taiwan

**Abstract**—In this paper, an antenna-mode-switch technique is proposed to reduce the array size for the DOA (direction-of-arrival) estimation. Conventional DOA estimation requires many elements of antenna array to achieve high resolution, and then suffers from large array size. To improve such disadvantages, this paper proposes an antenna-mode-switch technique to reduce the required number of array elements. Our results show that the required number of array elements will be greatly reduced by using the proposed technique. Furthermore, a bow-tie antenna design for implementing the proposed antenna-mode-switch technique is also proposed. The results prove that high-resolution and accurate properties of such a practical antenna design is very close to those of the ideal antenna mode.

## 1. INTRODUCTION

DOA (direction-of-arrival) estimation plays an important role in wireless communication systems. The goal is to find directions or even locations of signal sources. With the DOA information, the main beam of an antenna array can easily track the target source. Thus one can increase the signal-to-noise ratio (SNR), extend the radio coverage, enhance the privacy, and implement context-aware service in wireless communication systems [1–11]. Many techniques of DOA estimation have been introduced in [1]. Most of them need large amount of signal processing, such as eigenvalue decomposition of the incident signals and signal autocorrelation matrix calculation to achieve high resolution [12]. Great computation resources are utilized in the processes and they are not acceptable in mobile communication devices. Without loss of generality, the delay-and-sum DOA estimation

*Received 22 June 2012, Accepted 16 August 2012, Scheduled 5 September 2012*

* Corresponding author: Kun-Chou Lee (kclee@mail.ncku.edu.tw).

is considered in this paper. It is a simple and fast DOA algorithm and no eigenvalue decomposition process is required, so it consumes very few computations and is suitable to be realized on mobile devices. But conventional delay-and-sum DOA estimation requires many elements of antenna array to achieve high resolution, and then suffers from large array size. This then motivates us to develop a new technique to improve such disadvantages.

In this paper, an antenna-mode-switching technique is proposed to reduce the required array number of a smart antenna array. This study includes two parts, i.e., theoretical analysis and practical implementation. Initially, the theoretical analysis is first given. It utilizes the concept of array pattern diversity to get better diversity gain [13]. We expect to reduce the required element number of a smart antenna array by using antenna-mode-switching elements. Next, the practical implementation is proposed. A bow-tie antenna design is proposed to practically implement the antenna-mode-switching elements for the above smart antenna array. This design of antenna element can provide high resolution and accuracy. Therefore, the proposed antenna-mode-switching technique can be practically realized to reduce the array size and will be suitable for small mobile devices.

## 2. ARRAY ANALYSIS

Initially, the conventional delay-and-sum DOA [1] is briefly introduced. Figure 1 shows the structure of an $M$-element adaptive antenna array. In Figure 1, there are $D$ signal sources $S_1(t)$, $S_2(t)$, ..., $S_D(t)$ coming from directions of $\theta_1$, $\theta_2$, ..., $\theta_D$, respectively. The array output $y(t)$ can be expressed as [14]

$$y(t) = \bar{W}^H \cdot \bar{u}(t) \tag{1}$$

where the notation "$H$" denotes the Hermitian transpose. In (1), the weight vector $\bar{W}$ is defined as

$$\bar{W} = [W_1 \quad W_2 \quad \dots \quad W_M]^T \tag{2}$$

where $W_1$, $W_2$, ..., $W_M$ are weights of array elements, and the notation "$T$" denotes the transpose. The $\bar{u}(t)$ of (1) denotes the received signal and is given as

$$\begin{aligned} \bar{u}(t) &= [u_1(t) \quad u_2(t) \quad \dots \quad u_M(t)]^T \\ &= [\bar{a}(\theta_1) \quad \bar{a}(\theta_2) \quad \dots \quad \bar{a}(\theta_D)]_{M\times D} \cdot \begin{bmatrix} S_1(t) \\ S_2(t) \\ \vdots \\ S_D(t) \end{bmatrix}_{D\times 1} + \bar{n}(t) \end{aligned} \tag{3}$$

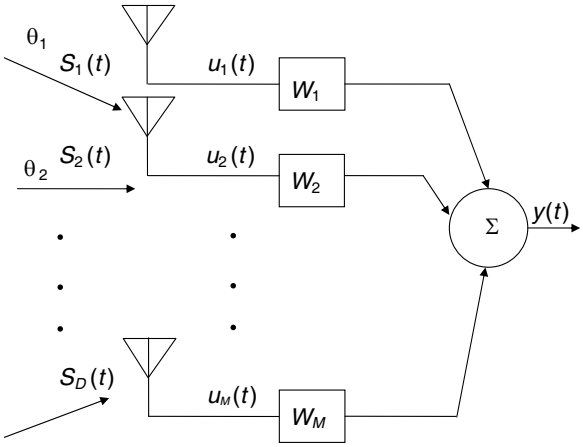


**Figure 1.** The structure of an $M$-element adaptive antenna array with $D$ signal sources.

where $\bar{a}(\theta_i)$, $i = 1, 2, \ldots, D$, is an $M$-element steering vector for the signal from direction $\theta_i$. In (3), the $\bar{n}(t)$ represents an additive Gaussian noise vector with zero mean. The array output power is

$$P = E\left[|y(t)|^2\right] = E\left[\left|\bar{W}^H \cdot \bar{u}(t)\right|^2\right] \tag{4}$$

where $E[\cdot]$ denotes the statistical average. Assume the array receives a signal from direction of $\theta_i$ $(1 \leq i \leq D)$. According to the delay-and-sum DOA estimation [1], the spatial spectrum of $P$ in (4) will have maximum (or peak) at $\theta = \theta_i$. The way to find is to plot the array output power with respect to scanned angles of directions. The angle which corresponds to the maximum array output power is the DOA of the incoming signal.

Although the conventional delay-and-sum DOA estimation given above is simple and efficient, it often requires many elements of antenna array to achieve high resolution. Consider a linear antenna array with element spacing of $\lambda/2$ ($\lambda$ is the wavelength). Assume there are two signals with equal SNR (signal-to-noise ratio) of 20 dB arriving from directions of $\theta = -10°$ and $\theta = 20°$. For simplicity, the mutual coupling effects between array elements are ignored in this paper. According to the conventional delay-and-sum method, the array output power with respect to scanned angles of directions under different number of array elements is plotted in Figure 2. The information contained in Figure 2 is further listed in Table 1. From Figure 2 and Table 1, it results that the error of delay-and-sum method is reduced as the number of array elements increases. In other words, the resolution of delay-and-

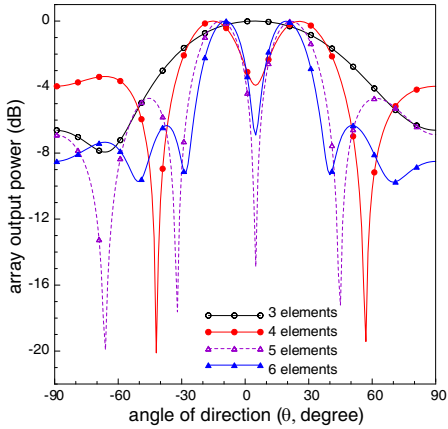


**Figure 2.** The array output power with respect to scanned angles of directions under different number of array elements by using the conventional delay-and-sum method.

**Table 1.** Information contained in Figure 2.

| No. of elements | signal from $\theta = -10°$ | | signal from $\theta = 20°$ | |
|---|---|---|---|---|
| | estimated DOA | error | estimated DOA | error |
| 3 | failed | failed | 5° | −15° |
| 4 | −15° | −5° | 26° | 6° |
| 5 | −12° | −2° | 22° | 2° |
| 6 | −9° | 1° | 19° | −1° |

sum method is improved as the number of array elements increases. In this example, the resolution of delay-and-sum DOA estimation will be unacceptable as the number of array elements is less than 6. To improve the resolution of DOA estimation, the number of array elements should be increased [16, 17] or correlated channels should be avoided by using array elements with different gain patterns [18]. However, the increase for number of array elements will also increase the array size and cost.

In order to diminish the disadvantages of conventional delay-and-sum method, an antenna-mode-switching technique is proposed in this study. In our treatment, each element of antenna array has two ideal modes in radiation pattern including ideal mode #1 and ideal mode #2. For each mode, the gain of the front lobe is 10 dBi larger

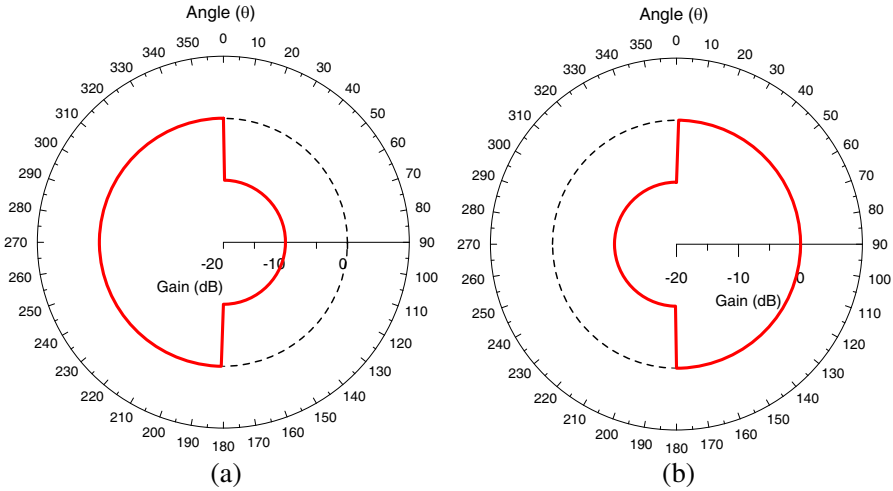


**Figure 3.** The antenna patterns of (a) ideal mode #1, and (b) ideal mode #2.

than that of the back lobe. The antenna patterns of the two modes are shown in Figure 3.

In Figure 3, the pattern "ideal mode #1" is for scanning the spatial region of $-90° < \theta < 0°$, whereas the pattern "ideal mode #2" is for scanning the spatial region of $0° < \theta < 90°$. In other words, each antenna element is switched to ideal mode #2 as the array scans within the spatial region of $0° < \theta < 90°$. Similarly, each antenna element is switched to ideal mode #1 as the array scans within the spatial region of $-90° < \theta < 0°$. The main benefit of such a two-mode radiating pattern is that it can reduce the interference from spatial region not being scanned. To illustrate such a benefit, we consider a linear antenna array with three elements spaced by $\lambda/2$, as shown in Figure 4.

As each element in Figure 4 is chosen as the dipole antenna with omni-directional radiation pattern in $X$-$Y$ plane, the array factor ($AF$) can be expressed as [15]

$$AF = 1e^{-j\beta\left(\frac{d}{2}\right)\sin\theta} + 1 + 1e^{j\beta\left(\frac{d}{2}\right)\sin\theta} = 1 + 2\cos\left(\beta\frac{d}{2}\sin\theta\right) \qquad (5)$$

where $d = \lambda$ and $\beta$ is wave number. As each antenna element is replaced by our sector antenna with radiation pattern "mode #2", the array factor is unchanged in directions of $0° < \theta < 180°$. But the array

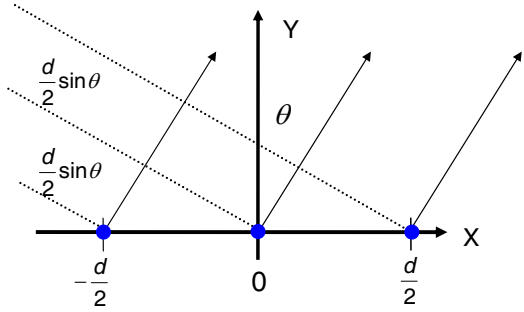


**Figure 4.** Schematic diagram of a linear antenna array with 3 elements ($d = \lambda$).

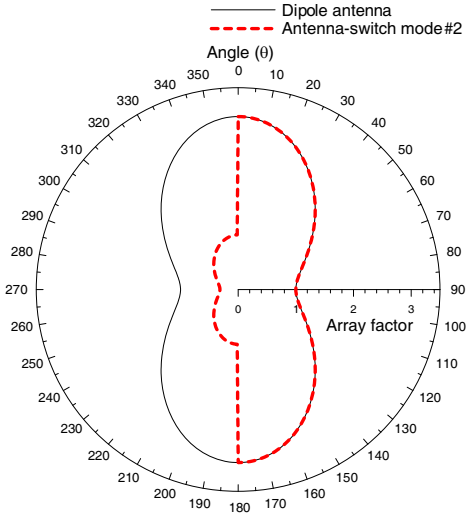


**Figure 5.** Array factor for a 3-element linear antenna array with each element chosen as conventional dipole antenna, or chosen as sector antenna of ideal mode #2.

factor in directions of $-180° < \theta < 0°$ becomes

$$AF = \frac{1}{\sqrt{10}} e^{-j\beta\left(\frac{d}{2}\right)\sin\theta} + \frac{1}{\sqrt{10}} + \frac{1}{\sqrt{10}} e^{j\beta\left(\frac{d}{2}\right)\sin\theta}$$
$$= \frac{1}{\sqrt{10}} \left[1 + 2\cos\left(\beta \frac{d}{2}\sin\theta\right)\right]. \quad (6)$$

Figure 5 shows the array factor for a 3-element linear antenna array with each element chosen as conventional dipole antenna, or chosen as

sector antenna of mode #2. In other words, Figure 5 shows the results of (5) and (6). From Figure 5, it clearly shows that interferences from spatial region $-180^\circ < \theta < 0^\circ$ can be greatly reduced as each array element is chosen as sector-antenna of ideal mode #2. Similarly, one can easily prove that interferences from spatial region $0^\circ < \theta < 180^\circ$ can be greatly reduced as each array element is chosen as sector-antenna of ideal mode #1. Therefore, an antenna array composed of sector-antenna elements (i.e., with antenna-mode-switching technique) will achieve better resolution than conventional dipole-antenna array due to low interferences.

Next, each element of the antenna array in Figures 1 and 2 is replaced by our sector antenna, i.e., with antenna-mode-switching technique. As mentioned above, the antenna array is assumed to contain 3 elements. By using the delay-and-sum DOA scheme with each element replaced by our sector antenna, the array output power with respect to scanned angles of directions for a 3-element array can be obtained. There are three examples given to illustrate our antenna-mode-switching technique. In the first example (case #1), there are two signals from directions of $\theta = -10^\circ$ and $\theta = 20^\circ$. Figure 6 shows the array output power with respect to scanned angles of directions for a 3-element array with antenna-mode-switching technique. For comparison, the result without antenna-mode-switching technique is also given in Figure 6. The information contained in Figure 6 is further listed in Table 2. From Figure 6 and Table 2, it results that the error of DOA estimation is greatly reduced as the antenna-mode-switching technique is added to the delay-and-sum scheme. In other words, the resolution of DOA estimation is greatly improved with the use of our antenna-mode-switching technique. From Figures 2 and 6, it results that the DOA resolution of "3-element array with antenna-mode-switching technique" is better than that of "6-element array without antenna-mode-switching technique". In other words, the use of antenna-mode-switching technique in delay-and-sum DOA estimation can greatly reduce the required number of array elements.

In order to make our antenna-mode-switching technique more reliable, additional examples are given. In the second example (case #2), there are two signals from directions of $\theta = -40^\circ$ and $\theta = 40^\circ$. All the other conditions are the same as those of the first example. The results are shown in Figure 7 and then further listed in Table 3.

In the third example (case #3), there are two signals from directions of $\theta = -80^\circ$ and $\theta = 80^\circ$. All the other conditions are the same as those of the first or the second example. The results are shown in Figure 8 and then further listed in Table 4. All the three examples (case #1, #2, #3) show that the DOA estimation resolution "with

**Table 2.** Information contained in Figure 6.

| | signal from $\theta = -10°$ | | signal from $\theta = 20°$ | |
|---|---|---|---|---|
| | estimated DOA | error | estimated DOA | error |
| without antenna-mode switch | failed | failed | 5° | −15° |
| with antenna-mode switch | −10° | 0° | 20° | 0° |

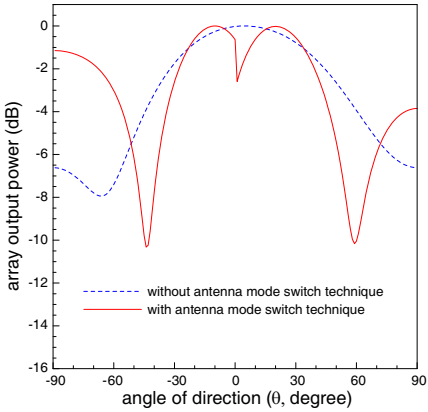


**Figure 6.** Case #1 (signals: $\theta = -10°$ and $\theta = 20°$) — the array output power with respect to scanned angles of directions for a 3-element array with and without antenna-mode-switching technique.

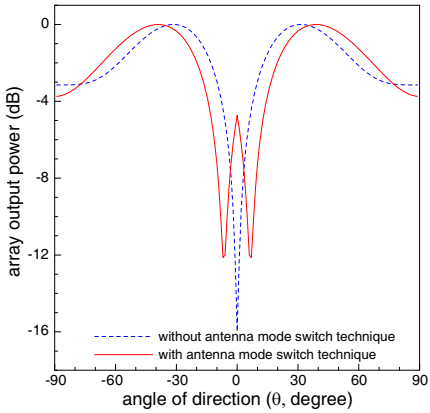


**Figure 7.** Case #2 (signals: $\theta = -40°$ and $\theta = 40°$) — the array output power with respect to scanned angles of directions for a 3-element array with and without antenna-mode-switching technique.

antenna-mode-switching technique" is better than that of "without antenna-mode-switching technique".

Note that all the three examples (Figure 6, Figure 7, and Figure 8) utilize only 3 elements in the antenna array and the results (accuracy & resolution) are better than most curves of Figure 2, which has 3, 4, 5, or 6 elements without proposed technique. For each example of the above analyses, the two signals come from directions of different sectors and the DOA estimation performance is very good. As the two

**Table 3.** Information contained in Figure 7.

| | signal from $\theta = -40°$ | | signal from $\theta = 40°$ | |
|---|---|---|---|---|
| | estimated DOA | error | estimated DOA | error |
| without antenna-mode switch | $-31°$ | $9°$ | $31°$ | $9°$ |
| with antenna-mode switch | $-39°$ | $1°$ | $39°$ | $1°$ |

**Table 4.** Information contained in Figure 8.

| | signal from $\theta = -80°$ | | signal from $\theta = 80°$ | |
|---|---|---|---|---|
| | estimated DOA | error | estimated DOA | error |
| without antenna-mode switch | $-89°$ | $9°$ | $89°$ | $9°$ |
| with antenna-mode switch | $-81°$ | $1°$ | $81°$ | $1°$ |

signals come from directions of the same sector, one can still obtain as good DOA estimation as different-sector signals by adding a phase shifter to each array element. Because this will result in a phase shift in each exponential term of Equations (5), (6) so that the two signals become "virtual" different-sector sources. Finally, the required number of antenna array for estimating the DOA is greatly reduced by our technique.

Next, the effect of array element number on proposed antenna-mode-switching technique is investigated. Figure 9 shows the array output power with respect to scanned angles of directions under different number of array elements by using the antenna-mode-switching technique. The information contained in Figure 9 is further listed in Table 5. From Figure 9, it reports that 3 elements are adequate in such examples to obtain accurate estimation of DOA. Therefore, the assumption of 3-element array in the above several examples is reasonable.

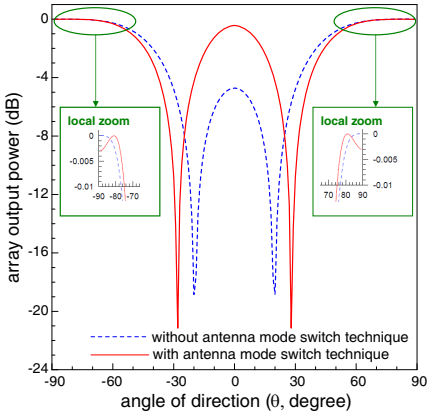


**Figure 8.** Case #3 (signals: $\theta = -80°$ and $\theta = 80°$) — the array output power with respect to scanned angles of directions for a 3-element array with and without antenna-mode-switching technique.

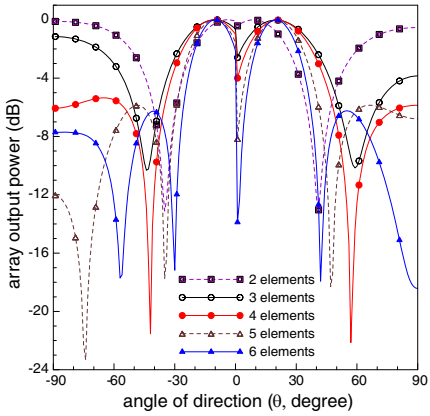


**Figure 9.** The array output power with respect to scanned angles of directions under different number of array elements by using the antenna-mode-switching technique.

**Table 5.** Information contained in Figure 9.

| No. of elements | signal from $\theta = -10°$ | | signal from $\theta = 20°$ | |
|---|---|---|---|---|
| | estimated DOA | error | estimated DOA | error |
| 2 | $-4°$ | $6°$ | $9°$ | $11°$ |
| 3 | $-10°$ | $0°$ | $20°$ | $0°$ |
| 4 | $-11°$ | $1°$ | $21°$ | $1°$ |
| 5 | $-10°$ | $0°$ | $19°$ | $1°$ |
| 6 | $-10°$ | $0°$ | $20°$ | $0°$ |

The above array analyses are implemented by using a personal computer (Acer Aspire One, CPU: 1.6 GHz Intel Atom N270) installed with Matlab 7.1 software. The computing time mainly depends on the complexity of DOA algorithms. In this study, the delay-and-sum DOA algorithm, which is simple and fast, is utilized for testing the antenna mode switch technique. The CPU time is approximately the same ($\approx 0.0469$ sec) for calculation with and without the antenna mode switch technique. It should be noted that the major advantage of antenna-modeswitching technique is to reduce the required number of array elements, but not the computing time.

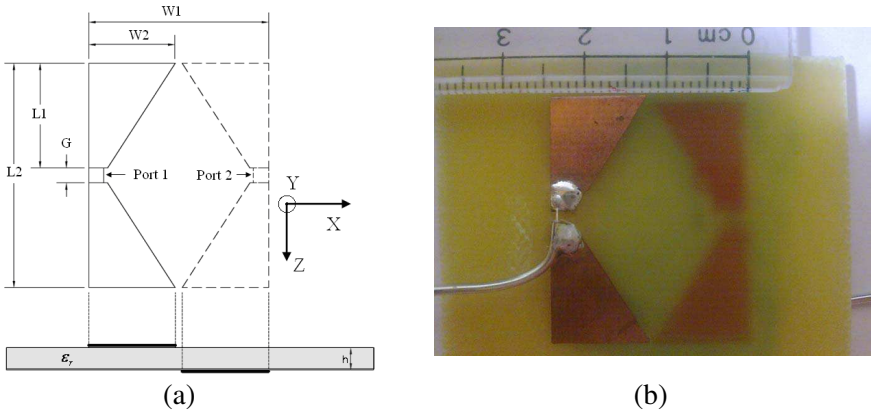


**Figure 10.** (a) Geometry of proposed bow-tie antenna design for one antenna element, and (b) photograph of antenna fabricated on FR-4 substrate.

## 3. IMPLEMENTATION OF ARRAY ELEMENT

The goal of this section is to find practical antenna design for implementing the proposed antenna-mode-switching technique, which has been theoretically analyzed in the previous section. For WLAN communications, antennas of 2.4 GHz are usually utilized in these devices. In order to design an antenna for such gain pattern at 2.4 GHz, bow-tie antennas are employed in some researches of DOA [19]. It is a compact size, wide band and high directivity antenna. Therefore the bow-tie antenna is a good choice for our goal. Figure 10 shows the geometry of proposed bow-tie antenna for one antenna element and its photograph on FR-4 substrate. In Figure 10, the practical antenna element is composed of two bow-tie components, i.e., component #1 and component #2. The whole element is small with size of $W_2 = 24\,\text{mm}$ and $L_2 = 30\,\text{mm}$. Such antenna design is experimentally realized on a FR-4 substrate ($\varepsilon_r = 4.4$, thickness $h = 1.4\,\text{mm}$). The component #1 is located at the top side of substrate and component #2 is located at the bottom side of substrate. As the switch is at mode #1, only port 1 is activated and radiation pattern at $XY$ plane can be obtained by both ANSYS HFSS software simulation and practical measurement. The simulation and measurement results are depicted in Figure 11(a). As the switch is at mode #2, only port 2 is activated and radiation pattern at $XY$ plane is shown in Figure 11(b).

Next, the pattern of antenna mode switch in Figure 3 (i.e., ideal case) is replaced by that of Figure 11 (practical antenna design). All

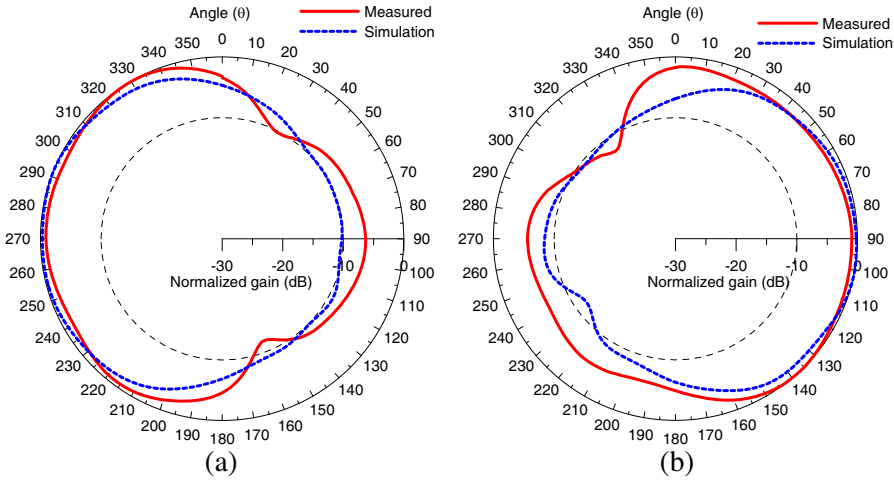


**Figure 11.** The simulated and measured antenna patterns for practical antenna design (a) mode #1, and (b) mode #2.

**Table 6.** Normalized antenna gains contained in Figure 3 and Figure 11.

| Angle | Gain of ideal antenna mode (dB) | | Simulated gain of practical antenna design (dB) | | Measured gain of practical antenna design (dB) | |
|---|---|---|---|---|---|---|
| | Mode #1 | Mode #2 | Mode #1 | Mode #2 | Mode #1 | Mode #2 |
| 20° | -10 | 0 | −7.12 | −3.83 | −9.00 | −2.02 |
| −10° | | −10 | −3.33 | −8.17 | −1.50 | −3.31 |
| 40° | −10 | 0 | −9.52 | −2.27 | −9.12 | −2.13 |
| −40° | | −10 | −1.16 | −10.47 | −.19 | −11.89 |
| 80° | −10 | 0 | −10.10 | −0.42 | −6.67 | −1.14 |
| −80° | | −10 | −0.18 | −8.85 | −0.91 | −6.06 |

gain information for the six directions of arrivals for signals mentioned in three examples of the previous section is listed in Table 6. The following three examples illustrate how the results of Section 2 vary as each array element is replaced by our practical antenna design.

In the first example (case #1), there are two signals from directions of $\theta = 20°$ and $\theta = -10°$. Figure 12 shows the array

**Table 7.** Information contained in Figure 12.

| | signal from $\theta = -10°$ | | signal from $\theta = 20°$ | |
|---|---|---|---|---|
| | estimated DOA | error | estimated DOA | error |
| Measure | $-10°$ | $0°$ | $21°$ | $1°$ |
| Simulation | $-10°$ | $0°$ | $20°$ | $0°$ |
| Ideal | $-10°$ | $0°$ | $20°$ | $0°$ |

**Table 8.** Information contained in Figure 13.

| | signal from $\theta = -40°$ | | signal from $\theta = 40°$ | |
|---|---|---|---|---|
| | estimated DOA | error | estimated DOA | error |
| Measure | $-39°$ | $1°$ | $39°$ | $1°$ |
| Simulation | $-38°$ | $2°$ | $38°$ | $2°$ |
| Ideal | $-39°$ | $1°$ | $39°$ | $1°$ |

output power with respect to scanned angles of directions for a 3-element array by using our practical antenna-mode-switching design (including simulation and experiments) as the array elements. For comparison, the result of using ideal antenna-mode-switching array elements is also given in Figure 12. The information contained in Figure 12 is further listed in Table 7. From Figure 12 and Table 7, it results that the difference of DOA estimation between ideal analysis and practical implementation is less than $1°$, which is very small and reasonable.

In the second example (case #2), the two signals come from directions of $\theta = 40°$ and $\theta = -40°$. Figure 13 shows the array output power with respect to scanned angles of directions for a 3-element array by using practical and ideal antenna-mode-switching array elements, respectively. The information contained in Figure 13 is further listed in Table 8. From Figure 13 and Table 8, it reports that the results by ideal analysis and practical implementation are very consistent.

Similarly, the third example (case #3) has two signals coming from directions of $\theta = 80°$ and $\theta = -80°$. Figure 14 shows the array output power with respect to scanned angles of directions for a 3-element array by using practical and ideal antenna-mode-switching array elements, respectively. The information contained in Figure 14 is further listed in Table 9. From Figure 14 and Table 9, it reports that the results by ideal analysis and practical implementation are very consistent.

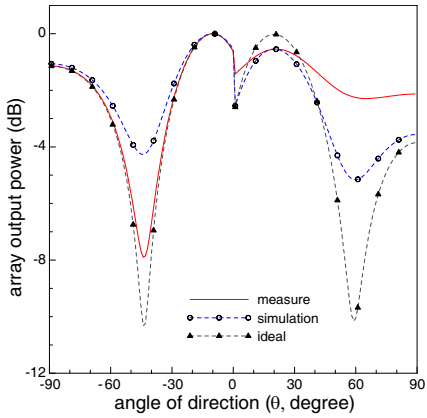


**Figure 12.** Case #1 (signals: $\theta = -10°$ and $\theta = 20°$) — the array output power with respect to scanned angles of directions for a 3-element array by using practical and ideal antenna-mode-switching array elements, respectively.

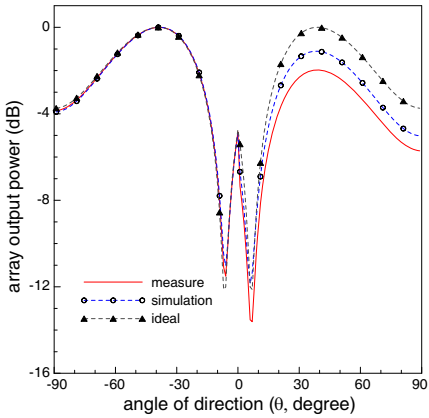


**Figure 13.** Case #2 (signals: $\theta = -40°$ and $\theta = 40°$) — the array output power with respect to scanned angles of directions for a 3-element array by using practical and ideal antenna-mode-switching array elements, respectively.

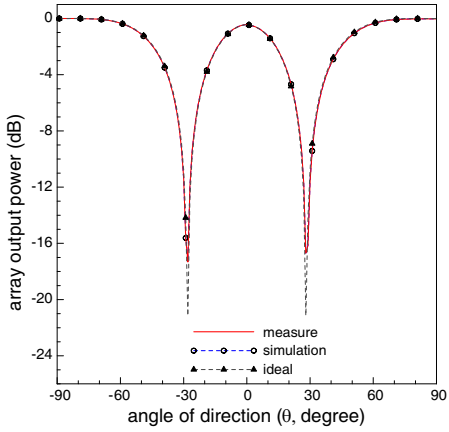


**Figure 14.** Case #3 (signals: $\theta = -80°$ and $\theta = 80°$) — the array output power with respect to scanned angles of directions for a 3-element array by using practical and ideal antenna-mode-switching array elements, respectively.

**Table 9.** Information contained in Figure 14.

| | signal from $\theta = -80°$ | | signal from $\theta = 80°$ | |
|---|---|---|---|---|
| | estimated DOA | error | estimated DOA | error |
| Measure | $-82°$ | $2°$ | $83°$ | $3°$ |
| Simulation | $-81°$ | $1°$ | $81°$ | $1°$ |
| Ideal | $-81°$ | $1°$ | $81°$ | $1°$ |

All the three examples (Figure 12, Figure 13 and Figure 14) have successfully utilized our practical antenna design to implement a 3-element smart antenna array. The results by using our practical antenna-mode-switching design are consistent with those of ideal analyses. In other words, the proposed idea of antenna mode switch for DOA estimation can be practically realized with high accuracy and excellent resolution.

## 4. CONCLUSION

In this paper, an antenna-mode-switching technique has been proposed to successfully improve disadvantages of delay-and-sum DOA estimation. Conventional omni-direction dipole antenna elements are replaced by antennas with particular radiation pattern to serve as the array elements and spatially filter the interferences. With the use of antenna-mode-switching technique, interferences from opposite half-space to desired signals are greatly reduced. Thus the resolution of DOA estimation is greatly improved due to the degrading of interferences. Therefore, the required number of array elements will be greatly reduced by using the proposed technique and the accuracy of DOA estimation is still very good. The reason why choosing the delay-and-sum DOA algorithm to test the proposed technique is that the delay-and-sum method is easy and fast to implement. It requires very little computing time and will be suitable for mobile devices. In fact, there is no limitation on choosing the DOA algorithm. In other words, our techniques can be applied to any other DOA algorithms since physically the interferences have been degraded. Our results show that the antenna-mode-switching technique can be practically implemented. Through the use of proposed technique, smart antenna arrays for DOA estimation will have the benefits of smaller size and better resolution. The proposed technique in this study can also be applied to many other topics in smart antennas or wireless communication systems [20–32].

## REFERENCES


1. Liberti, J. C. and T. S. Rappaport, *Smart Antenna for Wireless Communications IS-95 and Third Generation CDMA Applications*, Prentice Hall, NJ, 1999.
2. Jhang, J. Y. and K. C. Lee, "Array pattern optimization using electromagnetism-like algorithm," *AEU-Int. J. Electron. Commun.*, Vol. 63, 491–496, 2009.
3. Goossens, R. and H. Rogier, "Direction-of-arrival and polarization estimation with uniform circular arrays in the presence of mutual coupling," *AEU-Int. J. Electron. Commun.*, Vol. 62, 199–206, 2008.
4. El-Keyia, A. and T. Kirubarajan, "Adaptive beamspace focusing for direction of arrival estimation of wideband signals," *Signal Processing*, Vol. 88, 2063–2077, 2008.
5. Zha, H., "Fast algorithms for direction-of-arrival finding using large ESPRIT arrays," *Signal Processing*, Vol. 48, 111–121, 1996.
6. Yilmazer, N. and T. K. Sarkar, "2-D unitary matrix pencil method for efficient direction of arrival estimation," *Digital Signal Processing*, Vol. 16, 767–781, 2006.
7. Babu, K. V. S. and Y. Yoganandam, and V. U. Reddy, "Adaptive estimation of eigensubspace and tracking the directions of arrival," *Signal Processing*, Vol. 68, 317–339, 1998.
8. Wua, Y., G. Liaoa, and H. C. So, "A fast algorithm for 2-D direction-of-arrival estimation," *Signal Processing*, Vol. 83, 1827–1831, 2003.
9. Beygi, M. A. and A. Olfat, "Subspace based direction of arrival estimation of DS-CDMA signals using orthogonal projection," *Signal Processing*, Vol. 90, 926–932, 2010.
10. Verhaevert, J., E. V. Lil, and A. V. de Capelin, "Direction of arrival (DOA) parameter estimation with the SAGE algorithm," *Signal Processing*, Vol. 84, 619–629, 2004.
11. Agrawala, M. and S. Prasad, "Estimation of directions of arrival of wideband and wideband spread sources," *Signal Processing*, Vol. 87, 614–622, 2007.
12. Gotsis, K. A., K. Siakavara, and J. N. Sahalos, "On the direction of arrival (DOA) estimation for a switch-beam antenna system using neural networks," *IEEE Transaction on Antennas and Propagation*, Vol. 57, 1399–1411, 2009.
13. Kamarudin, M. R., Y. I. Nechayev, and P. S. Hall, "Onbody diversity and angle of arrival measurement using a pattern switch-

ing antenna," *IEEE Transaction on Antennas and Propagation*, Vol. 57, 964–971, April 2009.

14. Lee, K.-C., "A genetic algorithm based direction finding technique with compensation of mutual coupling effects," *Journal of Electromagnetic Waves and Applications*, Vo. l7, No. 11, 1613–1624, 2003.
15. Hansen, R. C., *Phased Array Antenna*, Wiley, New York, 1998.
16. Gross, F., *Smart Antennas for Wireless Communications with MATLAB*, McGraw-Hill, 2005.
17. Sarkar, T. K., M. Salazar-Palma, M. C. Wicks, and R. J. Bonneau, *Smart Antennas*, John Wiley & Sons, 2003.
18. Durgin, G. D., *Space-time Wireless Channels*, Prentice Hall, 2003.
19. Yeo, J. and J. Lee. "Miniaturized LPDA antenna for portable direction finding applications," *ETRI Journal*, Vol. 34, 118–121, February 2012.
20. Li, Y., Y. J. Gu, Z.-G. Shi, and K. S. Chen, "Robust adaptive beamforming based on particle filter with noise unknown," *Progress In Electromagnetics Research*, Vol. 90, 151–169, 2009.
21. Mouhamadou, M., P. Vaudon, and M. Rammal, "Smart antenna array patterns synthesis: Null steering and multi-user beamforming by phase control," *Progress In Electromagnetics Research*, Vol. 60, 95–106, 2006.
22. Zaharis, Z. D., C. Skeberis, and T. D. Xenos, "Improved antenna array adaptive beamforming with low side lobe level using a novel adaptive invasive weed optimization method," *Progress In Electromagnetics Research*, Vol. 124, 137–150, 2012.
23. Hong, T., M.-Z. Song, and Y. Liu, "RF directional modulation technique using a switched antenna array for communication and direction-finding applications," *Progress In Electromagnetics Research*, Vol. 120, 195–213, 2011.
24. Wounchoum, P., D. Worasawate, C. Phongcharoenpanich, and M. Krairiksh, "A switched-beam antenna using circumferential-slots on a concentric sectoral cylindrical cavity excited by coupling slots," *Progress In Electromagnetics Research*, Vol. 120, 127–141, 2011.
25. Wang, X., J.-F. Chen, Z.-G. Shi, and K. S. Chen, "Fuzzy-control-based particle filter for maneuvering target tracking," *Progress In Electromagnetics Research*, Vol. 118, 1–15, 2011.
26. Lee, J.-H., Y.-S. Jeong, S.-W. Cho, W.-Y. Yeo, and K. S. J. Pister, "Application of the Newton method to improve the accuracy of toa estimation with the beamforming algorithm and the music

algorithm," *Progress In Electromagnetics Research*, Vol. 116, 475–515, 2011.

27. Tian, B., D.-Y. Zhu, and Z.-D. Zhu, "A novel moving target detection approach for dual-channel SAR system," *Progress In Electromagnetics Research*, Vol. 115, 191–206, 2011.
28. Yang, P., F. Yang, and Z.-P. Nie, "DOA estimation with sub-array divided technique and interporlated esprit algorithm on a cylindrical conformal array antenna," *Progress In Electromagnetics Research*, Vol. 103, 201–216, 2010.
29. Jabbar, A. N., "A novel ultra-fast ultra-simple adaptive blind beamforming algorithm for smart antenna arrays," *Progress In Electromagnetics Research B*, Vol. 35, 329–348, 2011.
30. Mallipeddi, R., J. P. Lie, P. N. Suganthan, S. G. Razul, and C. M. S. See, "Near optimal robust adaptive beamforming approach based on evolutionary algorithm," *Progress In Electromagnetics Research B*, Vol. 29, 157–174, 2011.
31. Peng, H., Z. Yang, and T. Yang, "Calibration of a six-port receiver for direction finding using the artificial neural network technique," *Progress In Electromagnetics Research Letters*, Vol. 27, 17–24, 2011.
32. Liu, Y., Q. Wan, and X. Chu, "A robust beamformer based on weighted sparse constraint," *Progress In Electromagnetics Research Letters*, Vol. 16, 53–60, 2010.